



# PAH determination based on a rapid and novel gas purge-microsyringe extraction (GP-MSE) technique in road dust of Shanghai, China: Characterization, source apportionment, and health risk assessment



Xin Zheng<sup>a</sup>, Yi Yang<sup>a,\*</sup>, Min Liu<sup>a</sup>, Yingpeng Yu<sup>a</sup>, John L. Zhou<sup>b</sup>, Donghao Li<sup>c</sup>

<sup>a</sup> Key Laboratory of Geographic Information Science of the Ministry of Education, East China Normal University, Shanghai, China

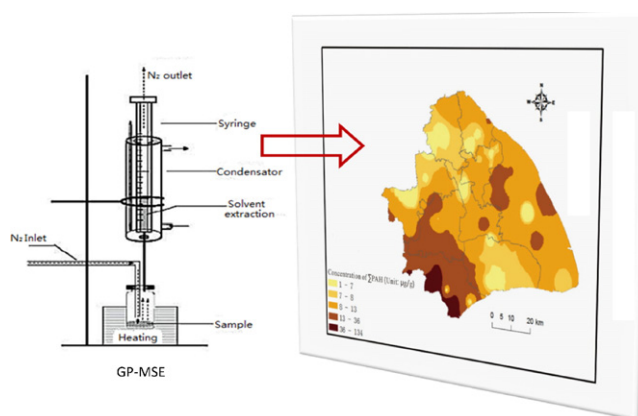
<sup>b</sup> State Key Laboratory of Estuarine and Coastal Research, East China Normal University, Shanghai, China

<sup>c</sup> Key Laboratory of Natural Resource of the Changbai Mountain and Functional Molecular of the Ministry of Education, Yanbian University, Yanji City, China

## HIGHLIGHTS

- GP-MSE cleanup technique was evaluated for PAH determination in dust samples.
- PAH distribution was characterized in the whole region of Shanghai.
- Both diagnostic ratio and PCA showed vehicle emission was the major source of PAHs.
- Six highly carcinogenic PAHs accounted for 98.6% of total BaPeq concentrations.

## GRAPHICAL ABSTRACT



## ARTICLE INFO

### Article history:

Received 18 November 2015

Received in revised form 17 March 2016

Accepted 17 March 2016

Available online 31 March 2016

Editor: D. Barcelo

### Keywords:

PAHs  
Road dust  
GP-MSE  
Source apportionment  
Shanghai

## ABSTRACT

A novel cleanup technique termed as gas purge-microsyringe extraction (GP-MSE) was evaluated and applied for polycyclic aromatic hydrocarbon (PAH) determination in road dust samples. A total of 68 road dust samples covering almost the entire Shanghai area were analyzed for 16 priority PAHs using gas chromatography–mass spectrometry. The results indicate that the total PAH concentrations over the investigated sites ranged from 1.04 µg/g to 134.02 µg/g dw with an average of 13.84 µg/g. High-molecular-weight compounds (4–6 rings PAHs) were significantly dominant in the total mass of PAHs, and accounted for 77.85% to 93.62%. Diagnostic ratio analysis showed that the road dust PAHs were mainly from the mixture of petroleum and biomass/coal combustions. Principal component analysis in conjunction with multiple linear regression indicated that the two major origins of road dust PAHs were vehicular emissions and biomass/fossil fuel combustions, which contributed 66.7% and 18.8% to the total road dust PAH burden, respectively. The concentration of benzo[*a*]pyrene equivalent (BaPeq) varied from 0.16 µg/g to 24.47 µg/g. The six highly carcinogenic PAH species (benz[*a*]anthracene, benzo[*a*]pyrene, benzo[*b*]fluoranthene, benzo[*k*]fluoranthene, dibenz[*a,h*]anthracene, and indeno[1,2,3-*cd*]pyrene) accounted for 98.57% of the total BaPeq concentration. Thus, the toxicity of PAHs in road dust was highly associated with high-molecular-weight compounds.

© 2016 Elsevier B.V. All rights reserved.

\* Corresponding author.

E-mail address: [yyang@geo.ecnu.edu.cn](mailto:yyang@geo.ecnu.edu.cn) (Y. Yang).

## 1. Introduction

Polycyclic aromatic hydrocarbons (PAHs) have been publicly accepted as one of the most ubiquitous class of anthropogenic organic pollutants. PAHs consist of multiple fused aromatic rings and are widely distributed in urban environments, such as the atmosphere, precipitation, urban surface road dust, soil, and sediment (Zhao et al., 2011; Huang et al., 2012). Several PAHs are mutagenic or carcinogenic (e.g., benzo[*a*]pyrene and benzo[*a*]anthracene). In particular, benzo[*a*]pyrene is always selected as an indicator of carcinogenic PAHs (Dahle et al., 2003).

In a city, most of these compounds are released into the environment primarily through anthropogenic activities. Dusts that are accumulated in impervious surfaces of urban roads can be subjected to various origins (e.g., weathered materials of road surfaces, vehicular emissions, tire debris) (Dong and Lee, 2009). As a strong sink of PAHs in an urban system, road dust has attracted great attention in recent decades (Fang et al., 2004; Boonyatumanond et al., 2007). PAHs in urban surface dusts are primarily derived from the deposition of PAHs containing particulates in the atmosphere and adsorption of emitted PAHs via direct exposure to vehicle exhaust emission (Zhang et al., 2008). During the rainy period, some surface dusts are washed off and finally enter the aqueous environment, thereby becoming a potentially significant source of PAHs in estuaries, surface water, sediments, and the food chain (Savinov et al., 2003).

For the determination of PAHs in a complex environmental matrix (e.g., dust), cleanup treatment, the most critical step, is necessary to ensure the accuracy of the experimental data. In a conventional PAH analytical process, approximately 60% to 80% of the experimental work is spent on the sample preparation (Yang et al., 2013). Numerous microextraction techniques for the determination of semivolatile organic compounds have been recently developed. Among these techniques, a novel technique termed gas purge-microsyringe extraction (GP-MSE) was initially introduced by Piao et al., 2011 and Yang et al., 2011. GP-MSE integrates sample extraction, cleanup, concentration, and introduction to analytical instruments such as GC-MS system. The advantage of this method is that it vastly decreases amount of solvent required and reduces the total process time in comparison to conventional chromatographic column cleanup, while increases the analysis efficiency. GP-MSE, a novel liquid phase microextraction technique, has been applied to various environmental matrix, including PAHs, alkylphenols (APs) and organic chlorine pesticides (OCPs) in plants and soils (Yang et al., 2011), phthalates esters (PAEs) in foodstuff (He et al., 2015), organophosphorus (OPPs) in edible fungus (Nan et al., 2015), APs in seafood (Yang et al., 2013), and PAHs in *Nostoc commune* and pine needles (Wang et al., 2013a). The extraction parameters that achieved the best performances in terms of extraction efficiency have been already systematically optimized in previous studies (Yang et al., 2011; Wang et al., 2013a). However, this technique has not been evaluated in the determination of PAHs in dust samples yet.

The metropolitan city of Shanghai, which has an area of 6340 km<sup>2</sup> and a population of >24 million, is located at the eastern continental shore of the Yangtze Estuary. With its rapid accelerating growth of motorization, population, and industrial activities, the amount of total suspended particles in Shanghai air is very high. The monthly average concentration of PM<sub>2.5</sub> was up to 82 µg/m<sup>3</sup>, and maximum monthly PM<sub>10</sub> concentration was 105 µg/m<sup>3</sup> in 2015 (Shanghai Environmental Protection Bureau, 2016). The city is also under the stress of airborne contaminants, such as PAHs (Feng et al., 2006). Previous studies conducting PAHs in Shanghai have been mainly focused on urban soil (Wang et al., 2013b), surface sediments (Liu et al., 2008), plant tissues (Wang et al., 2012), and gaseous and airborne particulate (Liu et al., 2015). Liu et al. (2007) had analyzed PAHs in Shanghai road dust. However, both the sampling area and the sampling number were limited. Therefore, information on PAHs in urban surface road dusts and their potential health risk is limited. In this study, road dust samples were

obtained from 68 sampling sites, which practically covered the whole region of Shanghai (information of sampling sites was described in Table S1). The objectives of the study were to (1) evaluate the potential of GP-MSE as a rapid and exhaustive sub-extraction (cleanup) technique for PAHs in road dust samples; (2) to conduct a comprehensive study on the PAH distribution in Shanghai road dust; (3) to identify their potential sources, and (4) to briefly assess their potential human health risks.

## 2. Materials and methods

### 2.1. Chemicals and standards

Eighteen polycyclic aromatic hydrocarbons (PAHs) standard mixtures, including naphthalene [Nap]; 2-methylnaphthalene [2-MNap]; 1-methylnaphthalene [1-MNap]; acenaphthylene [Acy]; acenaphthene [Ace]; fluorene [Flu]; phenanthrene [Phe]; anthracene [Ant]; fluoranthene [Flu]; pyrene [Pyr]; benzo[*a*]anthracene [BaA]; Chrysene [Chr]; benzo[*b*]fluoranthene [BbF], benzo[*k*]fluoranthene [BkF]; benzo[*a*]pyrene [BaP]; indeno[1,2,3-*cd*]pyrene [IcdP]; dibenz[*a,h*]anthracene [DBA]; benzo[*ghi*]perylene [BghiP] and internal standards (naphthalene-*d*8, anthracene-*d*10, phenanthrene-*d*10, chrysene-*d*10, and perylene-*d*12) were all purchased from Dr. Ehrenstrofer GmbH (Augsburg, Germany). The purity of standards was higher than 99%. Organic solvents, namely hexane, dichloromethane, and acetone, were all pesticide residue grade and purchased from ANPEL (Shanghai, China). The stock mixture standard solution of PAHs at a concentration of 10 mg/L was prepared in hexane. Standard working solutions of different concentrations were prepared by diluting the stock solutions with hexane. The stock solution of internal standard was prepared in hexane at 1000 mg/L and then diluted with hexane to 10 mg/L. All standard solutions were stored in the dark at 0–4 °C prior to use.

### 2.2. Sample collection

In this study, 68 road dust samples were collected from 20 August 2012 to 25 August 2012 (Fig. 1). Approximately 30 g of dust samples were collected along 100 m from each side of a road at each sampling site using plastic brushes and dustpans by gentle sweeping motion. The samples were passed through a 0.3 mm stainless sieve to remove large particles, hair, fibers, and other impurities, and then stored in a glass bottle for PAH extraction and analysis.

### 2.3. Sample preparation

PAHs were extracted using an accelerated solvent extractor (ASE 350, Dionex, Sunnyvale, CA, USA). Approximately 2 g of dust samples were extracted using a mixture of dichloromethane and acetone (1:1, v/v) at 100 °C and 10 MPa in static extraction mode for 15 min in duplicates. The extract was then solvent-exchanged into hexane and reduced to 1 mL under a gentle stream of nitrogen gas. Then five deuterated internal standards (naphthalene-*d*8, anthracene-*d*10, phenanthrene-*d*10, chrysene-*d*10, and perylene-*d*12) were added into the solvent extracts. The further cleanup of the extracts was performed using GP-MSE. The standard solutions of PAH mixture were spiked into the dust matrix at various levels to evaluate the recovery and linearity of the method. The blank dust sample was prepared by using Soxhlet extraction with dichloromethane/acetone (1:1, v/v) for 16 h to remove the PAHs.

### 2.4. GP-MSE

In this study, GP-MSE was used as a secondary extraction (cleanup step) procedure of PAHs from solvent extract of road dust sample (Yang et al. (2011)). Briefly, 10 µL of extract was spiked into the sample pool and tightly sealed with a polytetrafluoroethylene (PTFE) pad. A

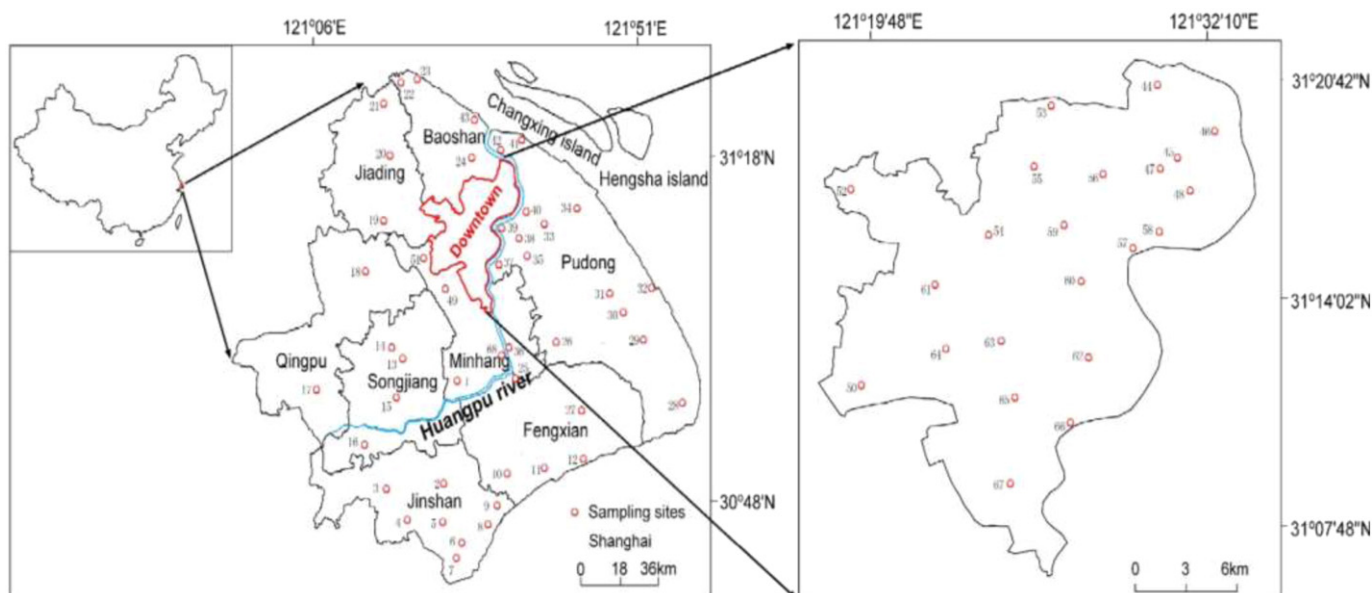


Fig. 1. Road dust sampling sites in Shanghai.

microsyringe (100  $\mu\text{L}$  volume, extraction syringe) without plunger was carefully inserted into the sample pool piercing through the PTFE pad. 10  $\mu\text{L}$  of hexane was added into the microsyringe as an extraction solvent. The extraction process was initiated after all the parameters were set (stated below). After a set extraction time, the microsyringe was rinsed three times with hexane and re-filled to 10  $\mu\text{L}$  (approximately 3  $\mu\text{L}$  to 6  $\mu\text{L}$  of hexane remained in the microsyringe after extraction). The extract was transferred into an inner tube (200  $\mu\text{L}$ ) of a 2 mL vial and 1  $\mu\text{L}$  extract solution was injected into GC–MS system for analysis. After each extraction cycle, the syringe was thoroughly washed by acetone twenty times and rinsed with hexane. The extraction parameters were set as follows: gas flow rate, 1.8 mL/min; extraction time, 2 min; heater temperature, 280  $^{\circ}\text{C}$ ; and extracting solvent temperature,  $-5^{\circ}\text{C}$ .

### 2.5. Traditional cleanup method

In order to evaluate results obtained by GP-MSE, the traditional silica-alumina chromatographic column was used as the comparison method. In brief, 10  $\mu\text{L}$  of extract for GP-MSE and 500  $\mu\text{L}$  taken from the same extract solvent was purified with a self-packed chromatographic column. The column cleanup procedure was conducted as follows: the column was packed with alumina (50–200 meshes, activated at 500  $^{\circ}\text{C}$  for 4 h), silica gel (100–200 meshes, activated at 130  $^{\circ}\text{C}$  for 12 h), and 2 g of anhydrous sodium sulfate (baked at 450  $^{\circ}\text{C}$  for 4 h) from bottom to top accordingly. The bulk mixture of alumina and silica gel was the ratio 1:2 in volume and both partially deactivated (4% and 5%, respectively) with distilled water. The first fraction was eluted with 15 mL hexane for aliphatic hydrocarbons which was discarded, and the second was subsequently eluted using a mixture of 70 mL dichloromethane/hexane (3:7, v/v). This fraction was concentrated by a rotary evaporator, solvent-exchanged into hexane, and reduced to 500  $\mu\text{L}$  under a gentle  $\text{N}_2$  purging for GC–MS analysis.

### 2.6. GC–MS analysis

The target compounds were determined by an Agilent 6890N GC coupled with an Agilent 5970 MS detector. A 30 m  $\times$  0.250 mm  $\times$  0.25  $\mu\text{m}$  DB-5 fused silica capillary column (Agilent Co., USA) in selected ion monitor (SIM) mode was used. Helium (purity of 99.999%) was used as the carrier gas at a constant flow of 1.0 mL/min. The ion source temperature was fixed at 270  $^{\circ}\text{C}$  and the split/splitless injector

temperature at 300  $^{\circ}\text{C}$ . The injection volume is 1  $\mu\text{L}$  in a splitless mode. PAH identification was based on a combination of retention times and relative abundances relative to five deuterated internal standards. Quantification of individual compounds was performed by comparing the peak areas with those of internal standards.

### 2.7. Data analysis

Principal component analysis (PCA) in conjunction with multiple linear regression analysis (MLR) were performed using SPSS 19.0 (IBM, USA). Graphs were plotted using Origin pro 8.0 (OriginLab, USA). Spatial distribution analysis of PAH was performed by ArcGIS 9.3 software (Esri, USA).

## 3. Results and discussion

### 3.1. Validation of the method

#### 3.1.1. QA/QC

Strict quality assurance and control measures were taken during all analytical procedures. For QA/QC, each sample was measured in duplicate. The relative standard deviations (RSDs) and relative average deviations for each compound were on average 12.3% and 7.9%, respectively. For every batch of 8–12 samples, a method blank, a blank spiked (standards solution spiked into solvent), and a matrix spiked (standards solution spiked into road dust samples) were also run. Method blank samples were analyzed by the same process as dust samples to determine any background contamination. PAHs almost were not detected in our method blank. The recoveries of the laboratory blank spiked samples ranged from 83.7% to 103.5% (RSD < 9.8%), and the recoveries of the matrix spiked samples were 81.2–111.8% (RSD < 14.6%). All the results were expressed on a dry weight basis.

#### 3.1.2. Evaluation of method performance

To evaluate the practical analytical performances and validate the proposed method, method quality parameters were evaluated in terms of limits of detection (LOD) and quantification (LOQ), reproducibility, linearity, precision and accuracy, and recovery of the GP-MSE technique for 18 PAH compounds. The performance of the method under the optimal conditions was shown in Table 1. The LOD and LOQ of the 18 PAHs were measured using diluted solutions of the PAHs

**Table 1**  
Quality parameters of GP-MSE technique.

Compound	LOD (pg/g)	LOQ (pg/g)	Linearity (R <sup>2</sup> )	Recovery (%)	RSD (%) (n = 6)	Recoveries of spiked blank dust samples (100 ng) (RSD) (%) (n = 5)	
						Intra-day	Inter-day
Nap	1.0	3.3	0.9812	92.9	7.5	85.8 (2.8)	83.8 (5.8)
1-MNap	1.0	3.3	0.9915	87.4	5.6	95.1 (4.0)	87.9 (3.4)
2-MNap	1.0	3.3	0.9926	89.8	4.8	88.6 (4.6)	92.3 (8.6)
Acy	0.5	1.7	0.9961	92.4	3.6	95.6 (1.6)	90.5 (8.9)
Ace	0.5	1.7	0.9932	95.8	5.5	97.8 (1.9)	96.7 (7.5)
Fl	0.3	1.0	0.9889	93.6	5.8	98.2 (2.4)	98.4 (7.8)
Phe	0.5	1.7	0.9978	86.5	5.3	88.4 (1.5)	95.1 (8.1)
Ant	1.0	3.3	0.9967	87.2	7.1	99.7 (3.7)	98.3 (5.4)
Flu	1.0	3.3	0.9948	92.2	1.8	87.8 (2.2)	89.1 (6.8)
Pyr	1.0	3.3	0.9813	96.5	6.1	95.8 (3.3)	97.2 (7.2)
BaA	1.5	5.0	0.9974	95.2	1.6	105.6 (3.1)	101.5 (3.4)
Chr	1.5	5.0	0.9968	90.3	5.8	100.8 (3.8)	97.6 (4.8)
BbF	1.5	5.0	0.9927	100.6	8.2	94.6 (2.1)	96.2 (2.5)
BkF	1.5	5.0	0.9905	105.2	4.4	93.5 (1.2)	87.8 (8.2)
BaP	1.8	6.0	0.9807	85.7	4.9	89.8 (1.1)	92.9 (7.4)
IcdP	2.0	6.7	0.9855	96.0	5.9	90.4 (3.6)	93.4 (7.2)
DBA	2.0	6.7	0.9871	104.5	5.3	92.6 (2.6)	87.8 (2.8)
BghiP	2.0	6.7	0.9891	102.8	4.3	94.4 (2.5)	103.5 (3.9)

LOD: limit of detection for S/N = 3.

LOQ: limit of quantification for S/N = 10.

RSD: relative standard deviation.

standards at a series of different concentrations, and seven replicates were set for each concentration. The LOD and LOQ were calculated as the analyte concentration giving a three and ten times signal-to-noise (S/N), respectively. LOD ranged from 0.3 pg/g to 2.0 pg/g, while LOQ were from 1.0 pg/g to 6.7 pg/g. To study the linearity of the method, calibration curves were established with five different levels of PAHs standard mixture (0.2, 0.4, 0.8, 2, and 5 ppm) were injected into sample matrix. The results showed that all of the target compounds exhibited good linearity with correlation coefficients varying from 0.9807 to 0.9978. The recovery and reproducibility of this method were investigated by six measurements of a 100 ng sample of standard mixture. The recoveries of the PAHs ranged from 85.7% to 105.2%, and their RSD (n = 6) values were between 1.6% and 8.2%. The precision and accuracy of the method was tested with analysis of a spiked blank dust samples that contain 100 ng of PAHs standard mixture, and were analyzed within one day with five replicates for the intra-day assay, and the five replicates were further determined in five different days over one week for the inter-day assay. The recoveries of PAHs calculated to be 83.8–103.5% with RSD values of 2.5–8.9% (inter-day) and 85.8–105.6% with RSD values of 1.1–4.6% (intra-day). The results of the experiments confirmed that the method described above was validated with high extraction efficiency, good linearity and reproducibility, and satisfactory precision and accuracy.

### 3.1.3. Application

The feasibility of the method was further tested for the analysis of some real road dust samples. First, recovery study of real samples were carried out by spiking three PAHs concentration levels (2, 40, and 100 ng) into dust samples. As shown in Table 2, for spiked dust samples, the recoveries of the 18 PAHs were satisfactory (81.5–112.5%), with RSD (n = 6) values of 1.3–12.6%. In addition, a comparison between results obtained by these two cleanup methods was carried out in several groups of real samples. For real samples, the results of the GP-MSE approach were similar to the results obtained from alumina-silica column. The ratios of results obtained by automatic GP-MSE and traditional method were close to 1 for most compounds, suggesting that the GP-MSE method is feasible, and it is a rapid and exhaustive secondary extraction technique of

PAH from road dust samples, with the improved reliability and analysis efficiency.

### 3.2. PAH concentration in road dusts

The total 16 EPA priority PAH concentrations ranged from 1.04 µg/g to 134.02 µg/g with a mean of 13.84 µg/g (Table 3). The highest PAH concentrations of 134.02, 82.29, and 83.40 µg/g were observed at sites 4, 6, and 7, respectively. These three sites were all located inside a petrochemical industrial park where a series of large-scale petroleum refining factories and coke plants operated. Meanwhile, the lowest PAH concentrations of 1.04, 1.16, 2.81, and 3.06 µg/g were recorded at sites 17, 31, 5, and 53, respectively. These sites were either located in a remote rural area or city green parks, and their low PAH concentrations could be attributed to low traffic density and absence of human and industrial activities.

As shown in Table S2, the average level of total EPA PAHs in this study was lower than those in central Shanghai area (Liu et al., 2007); Anshan, China (Han et al., 2009); Birmingham, UK (Harrison et al., 1996); Pasadena, USA (Rogge et al., 1993); Ulsan, Korea (Dong and Lee, 2009); and Cairo, Egypt (Hassanien and Abdel-Latif, 2008); while higher than those in Guangzhou, China (Wang et al., 2011); Tokyo, Japan (Khanal et al., 2014); and Bangkok, Thailand (Boonyatumanond et al., 2006). By comparing our results with other data reported globally, the measured total PAHs in our study was within the relatively low range.

As for the individual PAH composition, Flu was the dominant PAH in dust samples at 1.93 µg/g, followed by BbF, BghiP and BaP with average values of 1.62, 1.52, and 1.50 µg/g, respectively. These PAHs were closely related to vehicular emissions (Guo et al., 2003; Ravindra et al., 2008). This PAH profile was similar to the results found in Guangzhou (Wang et al., 2011). Moreover, Acy and Ace were the lowest PAHs in dust with mean values of 0.075 and 0.084 µg/g, respectively.

PAHs in road surface dust shared a common characteristic with the higher mass contribution of high-molecular-weight (HMW) PAHs (4–6 rings), which ranged from 77.85% to 93.62% (Fig. S1). The major source for HMW PAHs (BbF, BaP, IcdP, and BghiP) was gasoline vehicle emissions (Harrison et al., 1996; Zuo et al., 2007). The predominantly high fraction of HMW PAHs indicates that they mostly resulted from the combustion of petroleum fuels (Zakaria et al., 2002).



**Table 2**  
Comparison of GP-MSE and silica-alumina column (SAC) techniques using spiked dust samples.

Compounds	Spiked recovery (% RSD, n = 6)			Concentration (ng g <sup>-1</sup> ) (%RSD, n = 3)					
	Low levels (2 ng)	Medium levels (40 ng)	High levels (100 ng)	Group 1		Group 2		Group 3	
				GP-MSE	SAC	GP-MSE	SAC	GP-MSE	SAC
Nap	87.52 (6.7)	107.72 (8.7)	81.54 (4.3)	7.14 (8.8)	7.06 (4.7)	7.81 (10.0)	7.42 (8.1)	7.42 (8.1)	7.69 (6.0)
1-MNap	91.23 (4.8)	101.35 (6.5)	90.14 (5.5)	3.76 (9.9)	3.51 (7.1)	6.03 (11.7)	5.91 (9.0)	5.91 (9.0)	5.66 (0.3)
2-MNap	93.67 (11.4)	96.52 (9.4)	92.47 (5.7)	1.59 (7.7)	1.54 (1.6)	2.86 (8.4)	2.72 (8.9)	2.72 (8.9)	2.86 (4.7)
Acy	87.59 (9.6)	87.38 (3.2)	95.38 (8.5)	0.32 (6.3)	0.35 (15.8)	2.82 (1.9)	1.62 (3.7)	1.62 (3.7)	1.10 (3.1)
Ace	93.66 (5.2)	88.52 (6.6)	89.83 (8.3)	2.86 (13.5)	2.89 (10.4)	3.61 (10.0)	3.87 (4.8)	3.87 (4.8)	4.76 (0.6)
Fl	84.87 (2.2)	93.26 (7.5)	91.24(8.2)	1.78 (11.4)	2.02 (11.7)	8.90 (6.1)	8.71 (5.2)	8.71 (5.2)	11.37 (7.0)
Phe	100.27 (9.6)	87.88 (8.7)	88.69 (6.8)	11.41 (9.9)	12.69 (13.9)	82.59 (8.1)	80.81 (3.9)	80.81 (3.9)	50.83 (2.7)
Ant	82.98 (11.6)	92.65 (9.4)	85.81 (7.7)	0.68 (9.3)	0.73 (5.4)	8.47 (6.5)	6.19 (1.1)	6.19 (1.1)	7.96 (2.0)
Flu	105.67 (4.7)	91.23 (1.3)	95.03 (8.0)	9.78 (5.8)	10.46 (0.5)	115.55 (3.4)	107.48 (3.5)	107.48 (3.5)	77.67 (0.1)
Pyr	101.66 (3.8)	95.47 (8.7)	86.75 (7.8)	6.20 (5.5)	6.65 (2.2)	87.44 (3.5)	81.58 (3.6)	81.58 (3.6)	60.38 (0.9)
BaA	89.76 (8.4)	104.72 (11.9)	91.60 (9.3)	2.02 (3.0)	2.21 (1.1)	33.07 (7.5)	29.02 (4.6)	29.02 (4.6)	27.17 (5.1)
Chr	92.17 (8.9)	112.45 (8.6)	95.74 (7.6)	5.78 (2.9)	5.93 (3.1)	61.46 (8.5)	60.10 (3.8)	60.10 (3.8)	36.41 (1.7)
BbF	94.68 (7.6)	92.87 (11.2)	110.34 (6.4)	5.90 (10.4)	5.62 (8.0)	39.55 (2.7)	39.94 (2.3)	39.94 (2.3)	33.38 (1.1)
BkF	85.68 (3.1)	87.52 (5.8)	97.16 (5.5)	2.55 (6.2)	2.61 (5.7)	22.93 (10.1)	22.32 (2.7)	22.32 (2.7)	21.29 (2.6)
BaP	83.72 (12.1)	92.32 (7.3)	89.67 (7.7)	1.78 (6.0)	1.92 (4.1)	22.19 (5.4)	23.24 (4.9)	23.24 (4.9)	24.55 (0.8)
IcdP	84.56 (7.8)	84.62 (8.1)	98.48 (7.9)	1.34 (14.1)	1.57 (1.4)	16.96 (4.2)	22.30 (3.4)	22.30 (3.4)	19.50 (1.4)
DBA	100.16 (12.6)	96.33 (8.6)	101.92 (8.1)	1.84 (12.9)	0.49 (2.9)	6.24 (10.2)	7.14 (4.6)	7.14 (4.6)	6.07 (0.7)
BghiP	98.67 (9.6)	90.76 (7.6)	95.83 (8.9)	2.81 (3.1)	3.17 (8.4)	30.12 (7.3)	40.99 (4.1)	40.99 (4.1)	34.40 (1.7)

### 3.3. Spatial distribution of PAHs

The spatial distribution of  $\Sigma$  PAHs is plotted based on Kriging in Fig. 2. Some hot zones showed heavily polluted areas with high PAH concentrations. The southwestern part of Shanghai (sites 4, 6, and 7) showed the highest  $\Sigma$  PAH concentration. This area is a center of massive industrial establishments and all shared a high concentration of Flu, Pyr, BaA, Chr, and BkF which were tracers of coke plant (Kong et al., 2011). Sites 37, 38, and 39 were all located in the most prosperous commercial hub of Shanghai along the Huangpu River, which has an extremely busy traffic density. At those sites, BbF, BaP and BghiP were the three highest PAHs species which typically accounted for gasoline emission from vehicles (Guo et al., 2003). This commercial district exhibited the predominant effect of human activities on PAH contamination. The eastern part adjacent to the East China Sea (sites 30 and 32) was near an international airport where the number of flights accounted for

approximately 60% of that of total Shanghai airports. Ray et al. (2008) reported that aircraft engines have been demonstrated to emit considerable amounts of BaP (2–10 mg/min) and this is consistent with current study that BaP was the highest PAHs compound at site 32 where the sample was taken right outside the peripheral of airport. Sites 36 and 68, located near a heat and power plant, displayed a high loading of Phe, Flu, Pyr, BaA, Chr which were the indicators of coal combustion (Kong et al., 2011). This area represented the environmental burden of PAHs from coal combustion.

### 3.4. Source of PAHs in road dusts

#### 3.4.1. Diagnostic ratios

Diagnostic ratios have been extensively used as a classic convenient approach to help identify possible sources in several former studies (Yunker et al., 2002; Tobiszewski and Namieśnik, 2012). The ratios of LMW (2 + 3-ring PAHs)/HMW (4 + 5 + 6-ring PAHs) in the road dust samples ranged from 0.07 to 0.28 with a mean of 0.15. The ratio of LMW/HMW < 1, which indicates the predominance of the pyrogenic source (Wang et al., 2006; Yan et al., 2009). The mean values of IcdP/(Icdp + BghiP) and BaA/(BaA + Chr) were  $0.50 \pm 0.05$  and  $0.43 \pm 0.05$ , respectively (Fig. 3). According to Yunker et al. (2002), the value of BaA/(BaA + Chr) > 0.35 indicates coal, grass, and coal combustion. The value of IcdP/(Icdp + BghiP) between 0.2 and 0.5 indicates PAHs from petroleum combustion (liquid fossil fuels, vehicle, and crude oil). Thus, the diagnostic ratios imply that the PAHs were from mixtures of traffic emissions and biomass/coal combustions in this study area. This result agreed with the conclusion from a previous study, which reported that vehicle exhaust and coal combustion are major contributors to urban surface dust in central Shanghai areas (Liu et al., 2007). Moreover, BghiP is considered as a typical indicator of gasoline-powered automobile emissions (Guo et al., 2003). A strong correlation was observed between the concentrations of BghiP and total PAHs ( $R^2 = 0.996$ ,  $p < 0.0001$ ), thereby indicating that vehicular emission was a major source of PAHs in dust.

#### 3.4.2. PCA

The major advantage of PCA is that it simplifies the interpretation of complex systems and can represent the total variability of the original PAH data in a minimum number of factors that accounts for most of the variance of the original set (Larsen and Baker, 2003). In addition to the use of qualitative diagnostic ratios, PCA was used to further identify the specific sources of pollutant emissions in the studied region. The

**Table 3**  
PAH concentrations in surface road dusts of Shanghai ( $\mu\text{g/g}$ ).

	Aromatic ring	Mean	Minimum	Maximum	SD <sup>a</sup>
Nap	2	0.16	0.02	0.98	0.16
1-MNap	2	0.09	0.02	0.51	0.08
2-MNap	2	0.05	0.01	0.34	0.05
Acy	3	0.08	0.01	1.50	0.18
Ace	3	0.08	0.01	0.88	0.13
Fl	3	0.14	0.02	0.87	0.15
Phe	3	0.85	0.10	6.02	1.02
Ant	3	0.17	0.01	1.43	0.24
Flu	4	1.93	0.14	19.18	3.08
Pyr	4	1.41	0.10	14.31	2.25
BaA	4	1.11	0.07	13.47	1.99
Chr	4	1.00	0.08	8.50	1.38
BbF	5	1.62	0.11	16.46	2.71
BkF	5	0.66	0.05	7.89	1.19
BaP	5	1.50	0.10	15.21	2.40
IcdP	5	1.15	0.06	12.31	1.96
DBA	6	0.46	0.02	5.84	1.05
BghiP	6	1.52	0.09	13.29	2.32
LMW PAHs <sup>b</sup>		1.62	0.20	12.53	2.01
HMW PAHs <sup>c</sup>		12.36	0.82	126.46	20.33
$\Sigma$ PAHs <sup>d</sup>		13.98	1.02	138.99	22.34

<sup>a</sup> Standard deviation.

<sup>b</sup> Low molecular weight PAHs: 2–3 ring PAHs.

<sup>c</sup> High molecular weight PAH: 4–6 ring PAHs.

<sup>d</sup> Total PAH concentration.

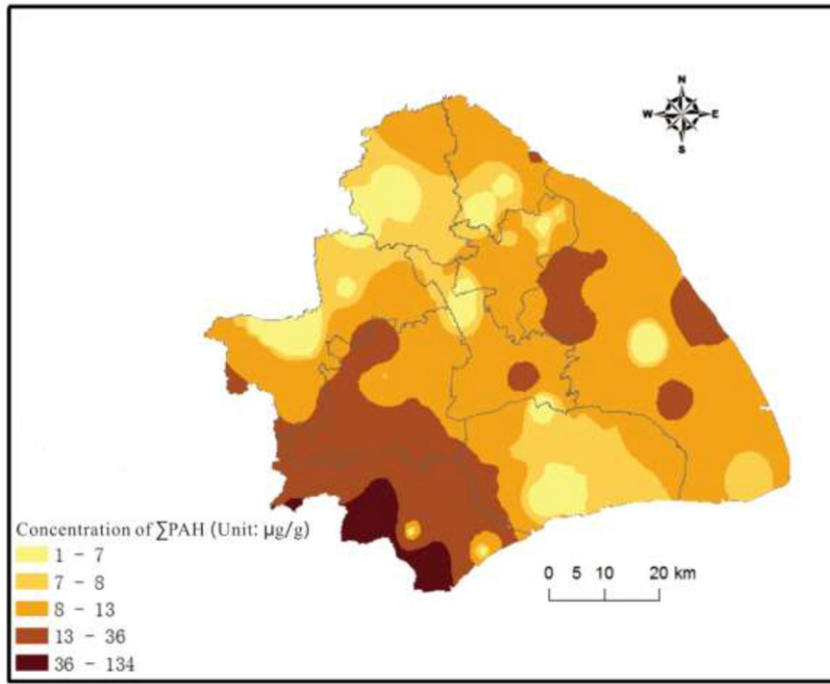


Fig. 2. Spatial distribution of  $\Sigma$ PAH concentrations in surface dusts of Shanghai.

results from PCA analysis on road dust PAHs are presented in Table 4. The variables with factor loading higher than 0.7 were marked in bold and considered relevant in the interpretation of each source factor. After varimax rotation, three principal components with eigenvalues >1 were extracted for the dust samples. The accumulative variances accounted for 95.62% of the total variability.

Factor 1 is responsible for 78.66% of the total variance. This factor was mostly associated with HMW (4–6 rings) PAHs, specifically Flu, Pyr, BaA, BbF, BkF, BaP, IcdP, DBA, and BghiP. A high factor loading of Flu, Pyr, and especially BghiP was considered for gasoline-powered vehicles (Khalili et al., 1995; Arinaitwe et al., 2012). Guo et al. (2003) also included BaA, BaP, BbF, BghiP, and IcdP as source markers for gasoline

emission. Other studies suggested that Flu and Pyr with high loading of BbF and BkF indicate diesel-powered vehicles (Shah et al., 2005; Ravindra et al., 2008). Consequently, this factor was attributed to vehicular emission sources. Several studies received the same conclusion that HMW PAHs indicate vehicular emission sources (Dong and Lee, 2009; Wang et al., 2011).

Factor 2 is responsible for 11.35% of the total variance. This factor was heavily weighted in Nap, 1-MNAP, and 2-MNAP with moderate loading of Flu and Phe. According to the literature, high loading of these PAH species were indicative of biomass combustion, as well as burned or unburned fossil fuels (Kim Oanh and Dung, 1999; Arinaitwe et al., 2012). Furthermore, Masclat et al. (1986) found that oil-fired

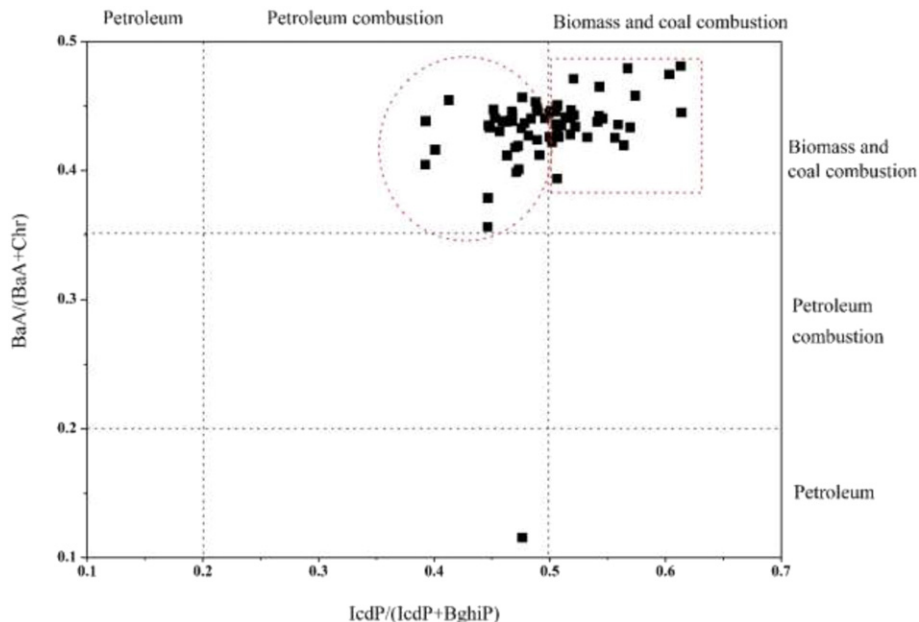


Fig. 3. Cross-plot for the isomeric ratios of BaA/(BaA + Chr) vs. IcdP/(IcdP + BghiP).

**Table 4**  
Rotated factor loading for PCA.

PAH	Factor 1	Factor 2	Factor 3
Percent of variance (%)	78.66	11.35	5.61
Nap	0.153	<b>0.908<sup>a</sup></b>	0.121
1-MNap <sup>b</sup>	0.371	<b>0.909</b>	−0.019
2-MNap <sup>b</sup>	0.247	<b>0.867</b>	−0.022
Acy	0.263	0.001	<b>0.956</b>
Ace	<b>0.888</b>	0.308	−0.192
Fl	<b>0.816</b>	0.538	−0.032
Phe	<b>0.888</b>	0.428	0.027
Ant	<b>0.898</b>	0.363	0.196
Flu	<b>0.942</b>	0.276	0.124
Pyr	<b>0.948</b>	0.269	0.105
BaA	<b>0.958</b>	0.261	0.018
Chr	<b>0.926</b>	0.218	0.286
BbF	<b>0.913</b>	0.180	0.360
BkF	<b>0.955</b>	0.185	0.212
BaP	<b>0.926</b>	0.173	0.316
IcdP	<b>0.941</b>	0.213	0.252
DBA	<b>0.804</b>	0.485	0.027
BghiP	<b>0.921</b>	0.225	0.271

<sup>a</sup> Factor loadings higher than 0.7 are marked in bold.

<sup>b</sup> In order to increase accuracy and efficacy of possible source interpretation by PCA, two additional source markers (1-Methylnaphthalene, 2-Methylnaphthalene) quantified in this study are also added to the variables.

power stations are predominately composed of two- and three-ring PAHs, specifically methylnaphthalenes and phenanthrene. Thus, this factor was designated as biomass and fossil fuel combustions.

Factor 3 is responsible for 5.61% of the total variance. This factor showed good correlation with only Acy. The correlations with the other variable loadings were generally lower than 0.3. Thus, this factor was unassigned because of the insufficient chemical information to allow a source interpretation. The existence of the third source is unclear, and may be attributed to the inherent inability of PCA to properly scale variables before analysis. Therefore, this factor was set as an unknown source.

#### 3.4.3. PCA/MLR

MLR analysis was performed based on the factor score matrix to determine the percent contribution of different sources to the total PAH burden in each dust sample. The model used in this study was described in detail elsewhere (Li et al., 2012). By performing a stepwise procedure, PC1 to PC3 were regressed against the standardized normal deviation of the total PAH concentration at 95% confidence level. The MLR equation is as follows:

$$Z = 0.942FS_1 + 0.265FS_2 + 0.025FS_3 \quad (R^2 = 0.999).$$

An excellent correlation was found between the predicted PAH concentrations obtained by the PCA/MLR model and the measured PAH concentrations ( $R^2 = 0.9995$ ,  $p < 0.0001$ ) (Fig. S2). This correlation reveals that PCA/MLR was effective in well estimating the PAHs. The mean percentage contribution of each source was calculated by the following equation:

$$\text{Mean contribution of source } i (\%) = 100 \times (B_i / \sum B_i).$$

Thus, the mean percent contribution was 66.7% for vehicular emissions, 18.8% for biomass and fossil fuel combustions, and 14.5% for the unknown source. Overall, 85.5% of the PAH burden was ascribed to either traffic-related source or biomass/fossil fuel combustions, which was consistent with the results from diagnostic ratio analysis. The contribution of source  $i$  to each road dust sample can be calculated by:

$$\text{Source } i (\mu\text{g/g}) = \text{mean} \sum \text{PAHs} \times B_i / \sum B_i + B_i \times FS_i \times \sigma_{\text{PAH}}$$

where  $FS_i$  is the factor score for factor  $i$ .  $\sigma_{\text{PAH}}$  is 21.55, and the mean total PAH is 13.94. The estimated contributions of each of the proposed sources for PAHs in each dust sample are shown in Fig. S3. The relative contributions between sources exhibited similar distribution patterns. The source from vehicle emission was dominant in most of the sites, especially sites 37, 38, 39, 45, 56, and 63, which were all located in downtown areas with busy traffic flow. Sites 4, 6, 7, 41, 42, and 43 showed the same pattern, and were near industrial areas with heavy diesel-powered trucks transporting cargos. However, few outlier sites showed a greater proportion of biomass and fossil fuel burning. This result was reasonable, in site 9, which was near a power-generation plant. Moreover, sites 14, 19, and 29 were located in rural villages, and sites 51 and 52 were sampled from green parks. The greater proportion of biomass and fossil fuel burning may have been caused by the open burning of grass, wood, and fallen leaves.

#### 3.5. Health risk assessment

Some PAHs have been recognized because of their documented mutagenicity and carcinogenicity (Sverdrup et al., 2002), such as BaA, BbF, BkF, BaP, DBA, and IcdP. In principle, the health risk assessment of PAHs can be assessed based on its BaP equivalent concentration (BaP<sub>eq</sub>), which has been extensively widely used by several relevant studies (Pufulete et al., 2004; Vojtisek-Lom et al., 2012). The toxicity of each PAH identified in the road dust samples was calculated by multiplying its concentration with the corresponding toxic equivalent factor, which represents the relative carcinogenic potency compared with that of BaP as proposed by Nisbet and LaGoy (1992). The toxic equivalent concentrations (TEQs) of PAH in road dusts varied from 0.16  $\mu\text{g/g}$  to 24.47  $\mu\text{g/g}$  with a mean of 2.44  $\mu\text{g/g}$ , which was considerably lower than that of Ulsan, Korea (16.47  $\mu\text{g/g}$ ) (Dong and Lee, 2009). The site with the highest TEQ was found around industrial establishments, which also had the highest total PAH concentration. A strong correlation between TEQs and total PAH concentration in road dust samples was observed ( $R^2 = 0.992$ ,  $p < 0.0001$ ), thereby revealing that high overall PAH concentration could lead to high toxicity of PAHs in road dust. The high carcinogenic potency of PAH species (BaA, BaP, BbF, BkF, DBA, and IcdP), which were classified as the most probable carcinogens by USEPA, generally accounted for >98% of the total BaP<sub>eq</sub> concentration. This significantly high proportion was also found in other studies, such as those in 96% in Liaoning Province, China (Kong et al., 2010) and 93% in Osaka, Japan (Hien et al., 2007).

People, living in cities, especially those living or working in environment with heavy traffic density or industrial activities, may face significant potential human health risks by exposure to toxic road dusts through different pathways (e.g., dermal contact, oral ingestion, and inhalation). The PAHs with high carcinogenic potency are usually derived from gasoline combustion, and they are more inclined to partition on the surface of solid particles because of their physicochemical characteristics. This finding should draw great attention because Shanghai is a highly urbanized and densely populated megacity.

#### 4. Conclusion

GP-MSE coupled with ASE and GC-MS was applied for the determination of PAHs in dust samples from Shanghai. GP-MSE was proven to be a fast and economical technique with satisfactory recovery and RSD ratios of PAHs, and thus recommended for wide application for the determination of PAHs in the environmental matrix. According to the results, the total PAH concentrations in road dust from Shanghai ranged from 1.04  $\mu\text{g/g}$  to 134.02  $\mu\text{g/g}$  with an average of 13.84  $\mu\text{g/g}$ , which was relatively lower than that of other studies worldwide. The most abundant PAH species were Flu, BbF, and BghiP with 1.93, 1.62, and 1.52  $\mu\text{g/g}$ , respectively. While the two, three-ring PAHs species were generally at lowest concentration with Acy (0.08  $\mu\text{g/g}$ ), Ace



(0.08  $\mu\text{g/g}$ ) and Fl (0.14  $\mu\text{g/g}$ ). The total PAH concentrations were highly correlated with the BghiP content, thereby indicating that vehicular emission was the dominant source of road dust PAHs. The HMW (4–6 rings) PAHs were the most predominant group and comprised 77.85% to 93.62% of the total PAH mass, thereby revealing a pyrogenic origin. Results obtained from the diagnostic ratios associated with PCA/MLR indicate that traffic emission and biomass/fossil fuel combustions were the two major possible sources, which contributed 66.7% and 18.8% to the total road dust PAH burden, respectively. The BaP<sub>eq</sub> concentration varied from 0.16  $\mu\text{g/g}$  to 24.47  $\mu\text{g/g}$  with a mean of 2.44  $\mu\text{g/g}$ . The six PAH species with high carcinogenic potency predominantly constituted the total BaP<sub>eq</sub> concentration, which could pose a health risk to people living in this area.

## Acknowledgements

This study was supported by a grant from the National Natural Science Foundation of China (No. 41130525 and 41522111 and 41271473), and the Fundamental Research Funds for the Central Universities. Additional support was provided by the Large Instruments Open Foundation of East China Normal University.

## Appendix A. Supplementary data

Supplementary data to this article can be found online at <http://dx.doi.org/10.1016/j.scitotenv.2016.03.124>.

## References

- Arinaitwe, K., Kiremire, B.T., Muir, D.C.G., Fellin, P., Li, H., Teixeira, C., Mubiru, D.N., 2012. Atmospheric concentrations of polycyclic aromatic hydrocarbons in the watershed of Lake Victoria, East Africa. *Environ. Sci. Technol.* 46, 11524–11531.
- Boonyatumanond, R., Wattayakorn, G., Togo, A., Takada, H., 2006. Distribution and origins of polycyclic aromatic hydrocarbons (PAHs) in riverine, estuarine, and marine sediments in Thailand. *Mar. Pollut. Bull.* 52, 942–956.
- Boonyatumanond, R., Murakami, M., Wattayakorn, G., Togo, A., Takada, H., 2007. Sources of polycyclic aromatic hydrocarbons (PAHs) in street dust in a tropical Asian megacity, Bangkok, Thailand. *Sci. Total Environ.* 384, 420–432.
- Dahle, S., Savinov, V.M., Matishov, G.G., Evenset, A., Naes, K., 2003. Polycyclic aromatic hydrocarbons (PAHs) in bottom sediments of the Kara Sea shelf, gulf of Ob and Yenisei Bay. *Sci. Total Environ.* 306, 57–71.
- Dong, T.T.T., Lee, B.-K., 2009. Characteristics, toxicity, and source apportionment of polycyclic aromatic hydrocarbons (PAHs) in road dust of Ulsan, Korea. *Chemosphere* 74, 1245–1253.
- Fang, G.-C., Chang, C.-N., Wu, Y.-S., Fu, P.P.-C., Yang, I.L., Chen, M.-H., 2004. Characterization, identification of ambient air and road dust polycyclic aromatic hydrocarbons in central Taiwan, Taichung, Sci. Total Environ. 327, 135–146.
- Feng, J., Hu, M., Chan, C.K., Lau, P.S., Fang, M., He, L., Tang, X., 2006. A comparative study of the organic matter in PM<sub>2.5</sub> from three Chinese megacities in three different climatic zones. *Atmos. Environ.* 40, 3983–3994.
- Guo, H., Lee, S.C., Ho, K.F., Wang, X.M., Zou, S.C., 2003. Particle-associated polycyclic aromatic hydrocarbons in urban air of Hong Kong. *Atmos. Environ.* 37, 5307–5317.
- Han, B., Bai, Z., Guo, G., Wang, F., Li, F., Liu, Q., Ji, Y., Li, X., Hu, Y., 2009. Characterization of PM10 fraction of road dust for polycyclic aromatic hydrocarbons (PAHs) from Anshan, China. *J. Hazard. Mater.* 170, 934–940.
- Harrison, R.M., Smith, D.J.T., Luhana, L., 1996. Source apportionment of atmospheric polycyclic aromatic hydrocarbons collected from an urban location in Birmingham, U.K. *Environ. Sci. Technol.* 30, 825–832.
- Hassanien, M.A., Abdel-Latif, N.M., 2008. Polycyclic aromatic hydrocarbons in road dust over Greater Cairo, Egypt. *J. Hazard. Mater.* 151, 247–254.
- He, M., Yang, C., Geng, R., Zhao, X., Hong, L., Piao, X., Chen, T., Quinto, M., Li, D., 2015. Monitoring of phthalates in foodstuffs using gas purge microsyringe extraction coupled with GC-MS. *Anal. Chim. Acta* 879, 63–68.
- Hien, T.T., Nam, P.P., Yasuhiro, S., Takayuki, K., Norimichi, T., Hiroshi, B., 2007. Comparison of particle-phase polycyclic aromatic hydrocarbons and their variability causes in the ambient air in Ho Chi Minh City, Vietnam and in Osaka, Japan, during 2005–2006. *Sci. Total Environ.* 382, 70–81.
- Huang, W., Wang, Z., Yan, W., 2012. Distribution and sources of polycyclic aromatic hydrocarbons (PAHs) in sediments from Zhanjiang Bay and Leizhou Bay, South China. *Mar. Pollut. Bull.* 64, 1962–1969.
- Khalili, N.R., Scheff, P.A., Holsen, T.M., 1995. PAH source fingerprints for coke ovens, diesel and gasoline engines, highway tunnels, and wood combustion emissions. *Atmos. Environ.* 29, 533–542.
- Khanal, R., Furumai, H., Nakajima, F., 2014. Toxicity assessment of size-fractionated urban road dust using ostracod *Heterocypris incongruens* direct contact test. *J. Hazard. Mater.* 264, 53–64.
- Kim Oanh, N.T., Dung, N.T., 1999. Emission of polycyclic aromatic hydrocarbons and particulate matter from domestic combustion of selected fuels. *Environ. Sci. Technol.* 33, 2703–2709.
- Kong, S., Ding, X., Bai, Z., Han, B., Chen, L., Shi, J., Li, Z., 2010. A seasonal study of polycyclic aromatic hydrocarbons in PM<sub>2.5</sub> and PM<sub>2.5–10</sub> in five typical cities of Liaoning Province, China. *J. Hazard. Mater.* 183, 70–80.
- Kong, S., Shi, J., Lu, B., Qiu, W., Zhang, B., Peng, Y., Zhang, B., Bai, Z., 2011. Characterization of PAHs within PM10 fraction for ashes from coke production, iron smelt, heating station and power plant stacks in Liaoning Province, China. *Atmos. Environ.* 45, 3777–3785.
- Larsen, R.K., Baker, J.E., 2003. Source apportionment of polycyclic aromatic hydrocarbons in the urban atmosphere: a comparison of three methods. *Environ. Sci. Technol.* 37, 1873–1881.
- Li, W.-H., Tian, Y.-Z., Shi, G.-L., Guo, C.-S., Li, X., Feng, Y.-C., 2012. Concentrations and sources of PAHs in surface sediments of the Fenhe reservoir and watershed, China. *Ecotoxicol. Environ. Saf.* 75, 198–206.
- Liu, M., Cheng, S.B., Ou, D.N., Hou, L.J., Gao, L., Wang, L.L., Xie, Y.S., Yang, Y., Xu, S.Y., 2007. Characterization, identification of road dust PAHs in central Shanghai areas, China. *Atmos. Environ.* 41, 8785–8795.
- Liu, Y., Chen, L., Jianfu, Z., Qinghui, H., Zhiliang, Z., Hongwen, G., 2008. Distribution and sources of polycyclic aromatic hydrocarbons in surface sediments of rivers and an estuary in Shanghai, China. *Environ. Pollut.* 154, 298–305.
- Liu, Y., Gao, Y., Yu, N., Zhang, C., Wang, S., Ma, L., Zhao, J., Lohmann, R., 2015. Particulate matter, gaseous and particulate polycyclic aromatic hydrocarbons (PAHs) in an urban traffic tunnel of China: emission from on-road vehicles and gas-particle partitioning. *Chemosphere* 134, 52–59.
- Masclet, P., Mouvier, G., Nikolaou, K., 1986. Relative decay index and sources of polycyclic aromatic hydrocarbons (PAHs). *Atmos. Environ.* 20, 439–446.
- Nan, J., Wang, J., Piao, X., Yang, C., Wu, X., Quinto, M., Li, D., 2015. Novel and rapid method for determination of organophosphorus pesticide residues in edible fungus using direct gas purge microsyringe extraction coupled on-line with gas chromatography-mass spectrometry. *Talanta* 142, 64–71.
- Nisbet, I.C.T., LaGoy, P.K., 1992. Toxic equivalency factors (TEFs) for polycyclic aromatic hydrocarbons (PAHs). *Regul. Toxicol. Pharmacol.* 16, 290–300.
- Piao, X., Bi, J., Yang, C., Wang, X., Wang, J., Li, D., 2011. Automatic heating and cooling system in a gas purge microsyringe extraction. *Talanta* 86, 142–147.
- Pufulete, M., Battershill, J., Boobis, A., Fielder, R., 2004. Approaches to carcinogenic risk assessment for polycyclic aromatic hydrocarbons: a UK perspective. *Regul. Toxicol. Pharmacol.* 40, 54–66.
- Ravindra, K., Sokhi, R., Van Grieken, R., 2008. Atmospheric polycyclic aromatic hydrocarbons: source attribution, emission factors and regulation. *Atmos. Environ.* 42, 2895–2921.
- Ray, S., Khillare, P.S., Agarwal, T., Shridhar, V., 2008. Assessment of PAHs in soil around the International Airport in Delhi, India. *J. Hazard. Mater.* 156, 9–16.
- Rogge, W.F., Hildemann, L.M., Mazurek, M.A., Cass, G.R., Simoneit, B.R.T., 1993. Sources of fine organic aerosol. 5. Natural gas home appliances. *Environ. Sci. Technol.* 27, 2736–2744.
- Savinov, V.M., Savinova, T.N., Matishov, G.G., Dahle, S., Naes, K., 2003. Polycyclic aromatic hydrocarbons (PAHs) and organochlorines (OCs) in bottom sediments of the Guba Pechenga, Barents Sea, Russia. *Sci. Total Environ.* 306, 39–56.
- Shah, S.D., Ogunyoku, T.A., Miller, J.W., Cocker, D.R., 2005. On-road emission rates of PAH and n-alkane compounds from heavy-duty diesel vehicles. *Environ. Sci. Technol.* 39, 5276–5284.
- Shanghai Environmental Protection Bureau, 2016. <http://www.sepb.gov.cn/fa/cms/shhj/index.htm> (Accessed in Mar. 2016).
- Sverdrup, L.E., Nielsen, T., Krogh, P.H., 2002. Soil ecotoxicity of polycyclic aromatic hydrocarbons in relation to soil sorption, lipophilicity, and water solubility. *Environ. Sci. Technol.* 36, 2429–2435.
- Tobiszewski, M., Namięśnik, J., 2012. PAH diagnostic ratios for the identification of pollution emission sources. *Environ. Pollut.* 162, 110–119.
- Vojtisek-Lom, M., Czerwinski, J., Leniček, J., Sekyra, M., Topinka, J., 2012. Polycyclic aromatic hydrocarbons (PAHs) in exhaust emissions from diesel engines powered by rapeseed oil methyl ester and heated non-esterified rapeseed oil. *Atmos. Environ.* 60, 253–261.
- Wang, X.-C., Sun, S., Ma, H.-Q., Liu, Y., 2006. Sources and distribution of aliphatic and polyaromatic hydrocarbons in sediments of Jiaozhou Bay, Qingdao, China. *Mar. Pollut. Bull.* 52, 129–138.
- Wang, W., Huang, M.-j., Kang, Y., Wang, H.-s., Leung, A.O.W., Cheung, K.C., Wong, M.H., 2011. Polycyclic aromatic hydrocarbons (PAHs) in urban surface dust of Guangzhou, China: status, sources and human health risk assessment. *Sci. Total Environ.* 409, 4519–4527.
- Wang, Z., Liu, Z., Yang, Y., Li, T., Liu, M., 2012. Distribution of PAHs in tissues of wetland plants and the surrounding sediments in the Chongming wetland, Shanghai, China. *Chemosphere* 89, 221–227.
- Wang, J., Yang, C., Li, H., Piao, X., Li, D., 2013a. Gas purge-microsyringe extraction: a rapid and exhaustive direct microextraction technique of polycyclic aromatic hydrocarbons from plants. *Anal. Chim. Acta* 805, 45–53.
- Wang, X.-T., Miao, Y., Zhang, Y., Li, Y.-C., Wu, M.-H., Yu, G., 2013b. Polycyclic aromatic hydrocarbons (PAHs) in urban soils of the megacity Shanghai: occurrence, source apportionment and potential human health risk. *Sci. Total Environ.* 447, 80–89.
- Yan, W., Chi, J., Wang, Z., Huang, W., Zhang, G., 2009. Spatial and temporal distribution of polycyclic aromatic hydrocarbons (PAHs) in sediments from Daya Bay, South China. *Environ. Pollut.* 157, 1823–1830.
- Yang, C., Piao, X., Qiu, J., Wang, X., Ren, C., Li, D., 2011. Gas purge microsyringe extraction for quantitative direct gas chromatographic-mass spectrometric



- analysis of volatile and semivolatile chemicals. *J. Chromatogr. A* 1218, 1549–1555.
- Yang, C., Zhao, J., Wang, J., Yu, H., Piao, X., Li, D., 2013. Water-based gas purge microsyringe extraction coupled with liquid chromatography for determination of alkylphenols from sea food *Laminaria japonica* Aresh. *J. Chromatogr. A* 1300, 38–42.
- Yunker, M.B., Macdonald, R.W., Vingarzan, R., Mitchell, R.H., Goyette, D., Sylvestre, S., 2002. PAHs in the Fraser River basin: a critical appraisal of PAH ratios as indicators of PAH source and composition. *Org. Geochem.* 33, 489–515.
- Zakaria, M.P., Takada, H., Tsutsumi, S., Ohno, K., Yamada, J., Kouno, E., Kumata, H., 2002. Distribution of polycyclic aromatic hydrocarbons (PAHs) in rivers and estuaries in Malaysia: a widespread input of petrogenic PAHs. *Environ. Sci. Technol.* 36, 1907–1918.
- Zhang, S., Zhang, W., Shen, Y., Wang, K., Hu, L., Wang, X., 2008. Dry deposition of atmospheric polycyclic aromatic hydrocarbons (PAHs) in the southeast suburb of Beijing, China. *Atmos. Res.* 89, 138–148.
- Zhao, J., Zhang, F., Xu, L., Chen, J., Xu, Y., 2011. Spatial and temporal distribution of polycyclic aromatic hydrocarbons (PAHs) in the atmosphere of Xiamen, China. *Sci. Total Environ.* 409, 5318–5327.
- Zuo, Q., Duan, Y.H., Yang, Y., Wang, X.J., Tao, S., 2007. Source apportionment of polycyclic aromatic hydrocarbons in surface soil in Tianjin, China. *Environ. Pollut.* 147, 303–310.